CRACK PROPAGATION IN FUNCTIONALLY GRADED MICROPOROUS THERMOVISCOPLASTIC MATERIALS

B. M. Love and R. C. Batra
Engineering Science and Mechanics, Virginia Polytechnic Institute and State University, Blacksburg, VA 24060 USA

Abstract

We study the initiation and propagation of a crack in a functionally graded (FG) plate comprised of tungsten (W) and nickel-iron (NiFe) and deformed in either plane strain tension or mode-II. Each constituent and the composite are modeled as isotropic thermoelastoviscoplastic material with the material behavior represented by the Johnson-Cook relation. Values of effective parameters for the composite are derived by the rule of mixtures. Two cases are studied; in one the volume fraction of W varies linearly from 0% at the left edge to 100% at the right edge and in the other the volume fractions are reversed. These are identified as NiFe2W and W2NiFe respectively. It is found that for mode-I deformations, plastic deformations at points near the crack-tip are infinitesimal and the crack propagation speed, C, varies with the crack length. For the W2NiFe FG plate, C continues to increase monotonically but for the other FG plate, it seems to approach a steady value. However, when deformed in mode-II, significant plastic deformations occur at points near the crack-tip; this work is underway and will be reported at the conference. The effect of the imposed nominal strain rate on the initiation and propagation of a crack has also been scrutinized.

1 INTRODUCTION

Modeling crack propagation during the solution of a transient problem by the finite element method (FEM) is very challenging since the crack initiation point and its path are to be determined as a part of the solution of the problem. Three strategies used to analyze fracture are: (i) introducing cohesive elements along inter-element boundaries that are weak in shear and tension but very strong in compression, (ii) representing a crack as two traction-free surfaces by placing two coincident but unconnected nodes at the crack initiation point and relieving tractions on the newly created crack surfaces, and (iii) reducing elastic constants in the failed region to zero and virtually eliminating these elements from the analysis of the problem. Each of these techniques has its advantages and disadvantages. An accurate modeling of the crack path and hence its speed of propagation requires a very fine FE mesh. Here we analyze transient plane strain coupled thermomechanical deformations of a FG microporous thermoelastoviscoplastic body and assume that a crack initiates at a point when either the effective stress there has reached $3\sigma_0$ or the porosity there equals 0.25. The body is either loaded axially to induce mode-I failure or in shear to simulate mode-II failure. As soon as a fracture criterion is met at a node N, two coincident but unconnected nodes are located there and joined to the node N*. The node N* is selected so that the gradient of the failure variable is least along the line NN*. Newly created crack surfaces are taken to be traction free and thermally insulated. Thus elastic unloading waves emanate from the crack surfaces and propagate into the body. By locating the crack tip at different times, we ascertain its speed.

2 FORMULATION OF THE PROBLEM

The balance laws for mass, linear momentum, moment of momentum, and the internal energy, are written in the Lagrangean or the referential description of motion. Elastic deformations, heat conduction and stresses due to thermal expansion are considered. Following assumptions are made in the analysis of the problem: (i) the strain rate tensor is additively decomposed into an elastic part, a plastic part and a thermal part; (ii) the Jaumann rate of the Cauchy stress tensor is a

linear function of the elastic part of the strain rate tensor; (iii) Young's modulus and the shear modulus decrease affinely to zero when the porosity approaches one; (iv) the porosity represents damage induced in the body; (v) the specific heat and the thermal conductivity are affine functions of porosity; (vi) a material point deforms plastically when the stress state satisfies Gurson's flow potential modified for its dependence upon the porosity and the dependence of the flow stress upon the plastic strain, plastic strain rate and temperature; the latter is assumed to be given by the Johnson-Cook relation; (vii) the associative rule of plasticity gives the plastic part of the strain rate tensor; (viii) Chu and Needleman's expression for the evolution of porosity applies; (ix) the rate of change of internal energy is a linear function of the first and the second time derivatives of temperature thereby resulting in a hyperbolic heat equation, and (x) each constituent and the equivalent homogenized medium are isotropic. Thus, both mechanical and thermal disturbances propagate at a finite speed. A complete set of equations and values of material variables used in computing results are given in [1].

We first analyzed transient deformations of a representative volume element (RVE) to evaluate effective properties of the composite as a function of the volume fraction of constituents. Values of elastic parameters so determined were found to match well with those given by the Mori-Tanaka scheme. However, values of parameters characterizing the plastic deformation could not be satisfactorily determined from deformations of the RVE. We thus use the rule of mixtures to evaluate values of all material parameters from those of the constituents and their volume fractions. It gives exact values of the mass density and the heat capacity, is simple to use, and often gives an upper bound for values of the composite.

We assume that the body is prismatic of uniform square cross-section, initial and boundary conditions are independent of the axial coordinate, and a plane strain state of deformation prevails in the body. When studying mode-I failure, an equal and opposite axial velocity is applied to the smooth top and bottom surfaces with a small horizontal sharp precrack present at its centroid. The thermomechanical deformations are assumed to be symmetric about the two centroidal axes. Thus deformations of only the right-half of the cross-section are analyzed with boundary conditions arising from the symmetry of deformations imposed at points on the vertical centroidal axis. The other vertical surface is taken to be traction free and thermally insulated. Normal velocity, null tangential tractions and zero heat flux are prescribed on the top and the bottom horizontal surfaces. The prescribed normal velocity increases linearly with time to its steady state value in 1 μs and is then held there. The body is initially at rest, at a uniform temperature and has zero initial porosity.

3 WEAK FORMULATION OF THE PROBLEM

The constitutive assumptions identically satisfy the balance of moment of momentum. Galerkin's method is used to derive a weak form of the balance of linear momentum, the balance of internal energy, equations expressing the Jaumann rate of the Cauchy stress tensor in terms of the elastic part of the strain rate tensor, and evolution equations for the effective plastic strain rate and the porosity, and of the velocity equaling the time rate of change of the present position. The Johnson-Cook relation is rewritten to express the effective plastic strain rate in terms of the effective stress, the effective plastic strain and the temperature. Also, an auxiliary variable equal to the time rate of change of temperature is introduced. Thus at each node there are thirteen unknowns, namely two components of the position vector, two components of velocity, four components of Cauchy's stress tensor, porosity, temperature, its rate of change, the effective plastic strain, and density. Galerkin's approximation incorporates natural boundary conditions and results in a system of coupled nonlinear ODEs for the unknowns. These ODEs are integrated by using the subroutine LSODE. During this integration process, essential boundary conditions are

imposed. The subroutine adjusts the time step adaptively to compute the solution within the prescribed accuracy.

4 COMPUTATION AND DISCUSSION OF RESULTS

The 10 mm x 10 mm cross-section has an initial sharp crack of length 1 mm at the vertical centroidal axis with the center of the crack coincident with the centroid of the plate. The plate is deformed at an average axial strain rate of either 200/s or 2,000/s. Values of Young's modulus, E, mass density, ρ, and Poisson's ratio, υ, for W and NiFe, and the speeds of the longitudinal wave in a bar and the Rayleigh waves are listed in the following Table.

Even though deformations are symmetric about the two centroidal axes, symmetry about the horizontal centroidal axis is exploited to reduce the problem size. The analysis of deformations of half plate facilitates using the node release technique for studying crack propagation. The FE mesh used to analyze the problem is

Table 1: Material parameters and wave speeds for nickel-iron and tungsten.

	Young's modulus (GPa)	Poisson's ratio	Mass density (kg/m^3)	Bar wave speed (m/s)	Acoustic impedance $(E\rho)^{0.5}$ (kg/m^2 s)	Rayleigh wave speed (m/s)
NiFe	255	0.29	9200	5265	48.44 $x10^6$	3035
Tungsten	406	0.20	17000	4887	83.08 $x10^6$	2874

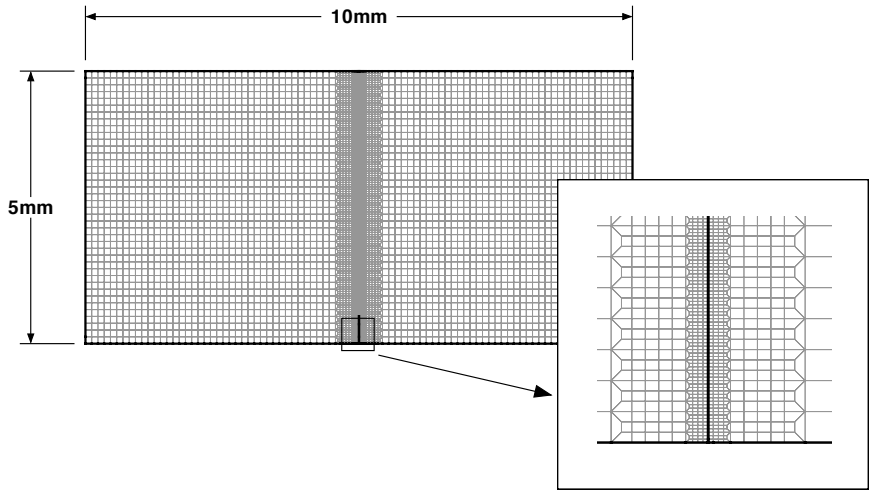

Figure 1: FE mesh for plane strain tensile deformations of pre-cracked plate.

depicted in Fig. 1. It consists of 17,444 4-node isoparametric quadrilateral elements with 1,080 elements along the axis of the crack. There are 108 elements behind the crack-tip and 972 ahead of it. The code has been validated by ensuring that the computed speed of an elastic wave is very close to the analytic value when E and ρ vary along the direction of propagation of the wave; the analytical solution is given in [2]. Once the failure criterion at a node has been met, that node is split into two essentially overlapping but unconnected nodes as described in the Introduction. Thus an elastic unloading wave emanates from the newly created crack surfaces and propagates into the body. The position of the crack tip at different times is determined and a polynomial is fit to the data. The first derivative of this polynomial fit gives C as a function of time. It was found that C so determined is very sensitive to the polynomial fit. Three curve fits with the coefficient of regression > 0.999 gave noticeably different values of C. Thus C at a point is taken to equal the slope of the least squares line through 21 points with 10 immediately preceding it and 10 immediately following it. The crack propagation speed, C, vs. the crack length for nominal strain rates of 200/s and 2,000/s is depicted in Figure 2; the Rayleigh wave speed is also plotted in the Figure. Freund's [3] analysis of crack propagation in an infinite homogeneous elastic body shows that the maximum crack propagation speed equals the Rayleigh wave speed; Eischen [4] has proved a similar result for nonhomogeneous materials. For the two homogeneous and the two FG plates, the crack propagation speed, C, is higher when the nominal strain rate is 2,000/s than that at a nominal strain rate of 200/s. For the W plate deformed at 200/s, C increases as the crack propagates to the right edge of the plate but at the higher strain rate of 2,000/s, it soon approaches a steady value that is a little less than the Rayleigh wave speed. For a NiFe plate deformed at 2,000/s, the crack propagates to the right for a little while and then a large region of the plate ahead of the crack suddenly shatters as indicated by the maximum principal tensile stress exceeding $3\sigma_0$. It is signified in Fig. 2b by the sudden drop in the crack propagation speed C. For W2NiFe FG plate, C continues to increase with the crack length, is always less than the Rayleigh wave speed when the plate is deformed at 200/s but approaches the Rayleigh wave speed when the nominal strain rate is 2,000/s. However, for the NiFe2W FG plate, even though the Rayleigh wave speed decreases monotonically with the distance from the left edge because of the spatial variation in the material properties, the computed crack speed C first increases and approaches essentially a steady value after the crack has propagated a certain distance.

We have plotted in Figure 3 the variation of the axial load as the crack propagates to the right. At a strain rate of 200/s, the crack propagation is stable in both pure W and W2NiFe FG plates as signified by the increase in the axial load except when the crack has propagated to a point near the right edge. However, at the higher strain rate of 2,000/s, the crack propagation seems to be unstable in the beginning and becomes stable once the crack length equals approximately one-half of the plate width. A similar situation occurs in pure NiFe and NiFe2W FG plates except that a large chunk of material ahead of the crack suddenly fails in the pure NiFe plate deformed at a nominal strain rate of 2,000/s.

5 CONCLUSIONS

We have analyzed the initiation and propagation of brittle fracture in homogeneous and functionally graded plates deformed in plane strain tension at nominal strain rates of 200 and 2,000/s. It is found that the crack propagation is stable at the strain rate of 200/s but is unstable at the higher strain rate of 2,000/s till the crack length equals one-half the plate width. When the crack length in a NiFe plate deformed at 2,000/s equals one-half the plate width, a large region of the material ahead of the crack tip fails instantaneously signifying shattering of the plate. For the finite size plate studied here, the maximum computed crack speed is almost equal to the Rayleigh wave speed. For an FG plate, the Rayleigh wave speed varies with the position as depicted in Figure 2.

Acknowledgements: This work was partially supported by the NSF grant CMS0002849, the ONR grant N00014-98-1-0300, the ARO grant DAAD19-01-1-0657 and the AFOSR MURI to Georgia Institute of Technology with a subcontract to Virginia Polytechnic Institute and State University.

6 REFERENCES

1. Batra, R.C., Love, B.M., Adiabatic shear bands in functionally graded materials, J. of Thermal Stresses (in press).
2. Chiu, T.C., Erdogan, F., One-dimensional wave propagation in a functionally graded medium, J. of Sound and Vibration, 222, 453-487, 1999.
3. Freund, L.B., Crack propagation in an elastic solid subjected to general loading – III. Stress wave loading, J. of the Mechs. and Physics of Solids, 21, 47-61, 1973.
4. Eischen, J.W., Fracture of nonhomogeneous materials, Int. J. of Fracture, 34, 3-22, 1987.

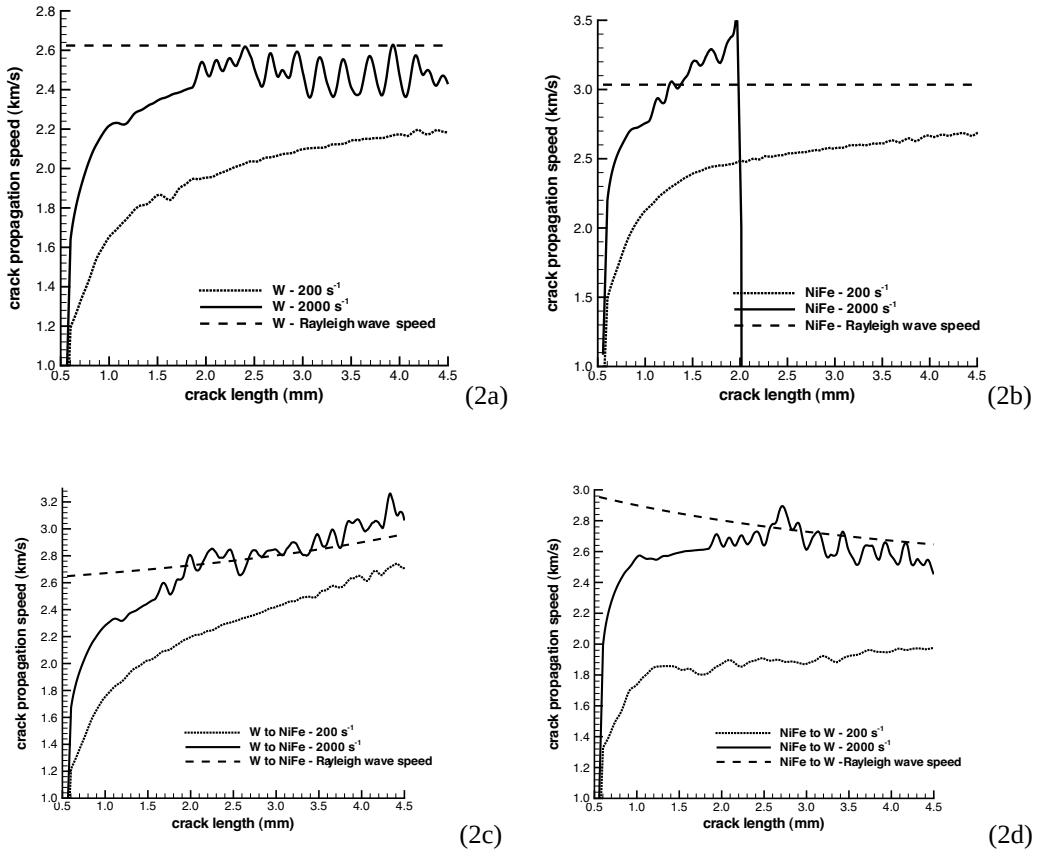

Figure 2: Crack propagation speed versus crack length at nominal rates of 200/s and 2000/s for (a) tungsten, (b) nickel-iron, (c) W2NiFe, and (d) NiFe2W.

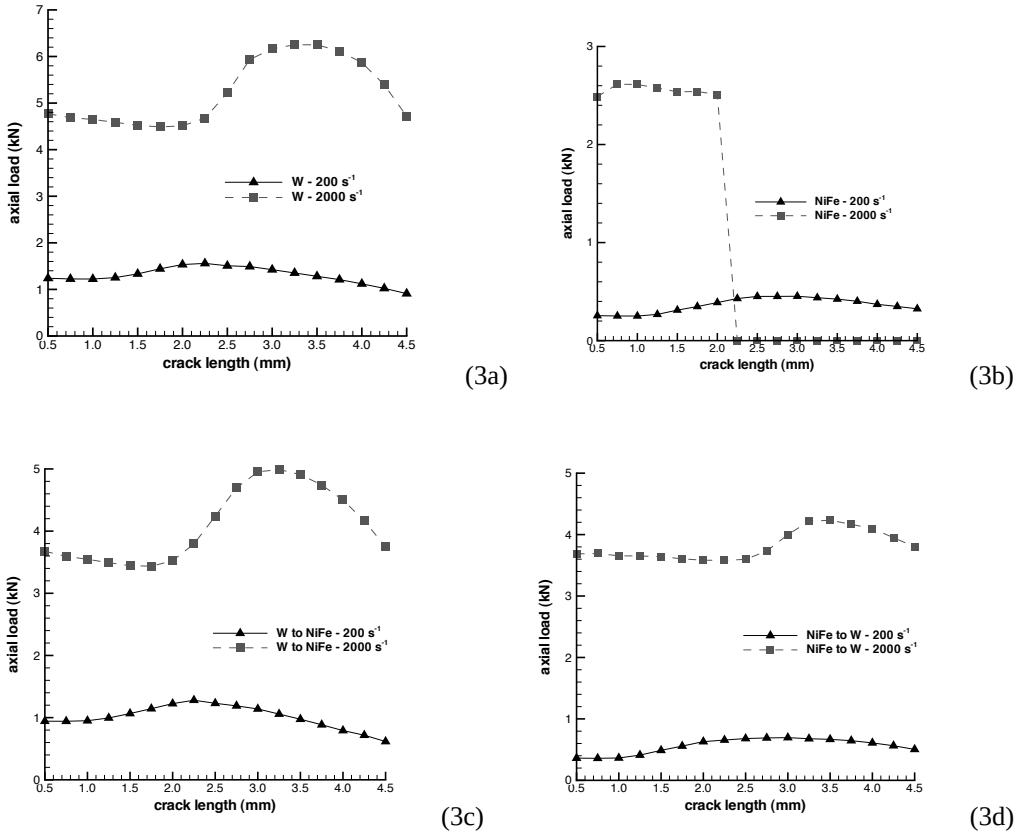

Figure 3: Axial load versus crack length at nominal strain rates of 200/s and 2000/s for (a) tungsten, (b) nickel-iron, (c) W2NiFe, and (d) NiFe2W.